6-1-1977

Direct Measurement of the Optical Modulation Transfer Function of Non-Developed Emulsions

Glen Elie

School of Photographic Arts and Sciences
Rochester Institute of Technology
Rochester, New York

CERTIFICATE OF APPROVAL

MASTER'S THESIS

This is to certify that the Master's Thesis of

Glen C. Elie

with a major in Photographic Science and Instrumentation has been approved by the Thesis Committee as satisfactory for the thesis requirement for the Master of Science degree at the convocation of

Thesis Committee: M. Abouelata
Thesis adviser

Name Illegible
Graduate adviser

Burt H. Carroll
Director or designate

DIRECT MEASUREMENT OF THE OPTICAL MODULATION TRANSFER FUNCTION OF NON-DEVELOPED EMULSIONS

by

Glen C. Elie

A thesis submitted in partial fulfillment of the requirements for the degree of Master of Science in the Photographic Science and Instrumentation Division of the School of Photographic Arts and Sciences

June, 1977

Thesis adviser: Professor Mohamed F. Abouelata

ACKNOWLEDGEMENTS

I would like to express my sincere thanks to my adviser, Professor M. Abouelata, for his constant support and guidance throughout this thesis, and to Professor J. Carson for his valuable assistance in the preliminary testing of the equipment. I am also very grateful to Dr. B. Carroll for his suggestions concerning the analysis of the experimental results.

TABLE OF CONTENTS

LIST OF TABLES

LIST OF FIGURES

ABSTRACT

A new procedure for measuring the MTF of non-developed emulsions is discussed, which uses a coherent energy source and interference system to produce sinusoidal fringes on a film sample. The transmitted light is projected onto the scanning slit of a photomultiplier, and its variations registered on a chart recorder. Measurements are taken directly from the traces of the irradiance distribution to calculate the optical part of the MTF of the sample. This system does not require development of the film, and is therefore free of the non-linearities inherent in traditional test methods.

Results are obtained for Kodak Panatomic-X, Kodak High Contrast Copy, and Kodalith Ortho Type 3 films, and compared where possible to the MTF derived from standard techniques. The MTF found from this study is that of the light distribution in the undeveloped emulsion layer, while the conventional method gives the MTF of the developed film. Adjacency effects in development cause the two methods to produce different results. It is concluded that this system is capable of producing excellent results for some types of films. Recommendations are made for improvement of the apparatus to render the procedure more universally suitable.

INTRODUCTION

Image quality is a concept often referred to in general terms, but determining an overall basis for any judgement is a difficult if not impossible task. Because of the number of different film characteristics involved, image quality depends on which of these is being assessed. A perfect reproduction in all respects is not possible, so the photographer must compromise by choosing a film which will best represent the subject, knowing that this may mean only a second best reproduction of another area. A photograph containing sharp architectural lines may appear as clear as the original scene, while an inscription on the side of the same building is almost illegible. It is important to be able to rate the performance of films with respect to their characteristics, and to do so, standard tests are required. This thesis is concerned with one of these tests, the optical part of the Modulation Transfer Function.

The evaluation of an image occurs at different levels, and has as its culmination the subjective opinion, itself dependent on image content. In this section, the basic levels of image evaluation will be reviewed and interrelated, showing their progression towards the final subjective appraisal. Graphically, the levels may be represented as

follows:

Line Spread Function (LSF)	Basis of all other tests, yet difficult to relate to final image.
Modulation Transfer Function	Spatial frequency response curve, used to measure contrast reduction of targets.
Resolution, Acutance	Each expressed as single number related to specific areas of MTF curve. Resolution depends on shape of the neck of the LSF, and Acutance depends on the shape of the base of the LSF[1].
Subjective Opinion	Visual appearance evaluated by observer without special equipment.

Each level leads to the one below, with the basic requirement being that the system is struck by light. Just how a photographic emulsion reacts to a point of light is the first concern, since all more complicated sources are made up of a series of points, and are therefore based on this[2].

When an infinitesimal surface area of film is exposed to light, one of several things can happen to the photons entering the emulsion. They may be absorbed by the first grain they encounter. They may be reflected to a second or higher number grain before being absorbed. Or they may pass

out of the emulsion without being absorbed at all. As the photons travel through the film, they are reflected sideways to a certain extent. This sideways scatter will be approximately symmetrical in photographic emulsions. If we took a cross-section of the film through the location where it was light-struck, we would see something as in Figure 1. Moving

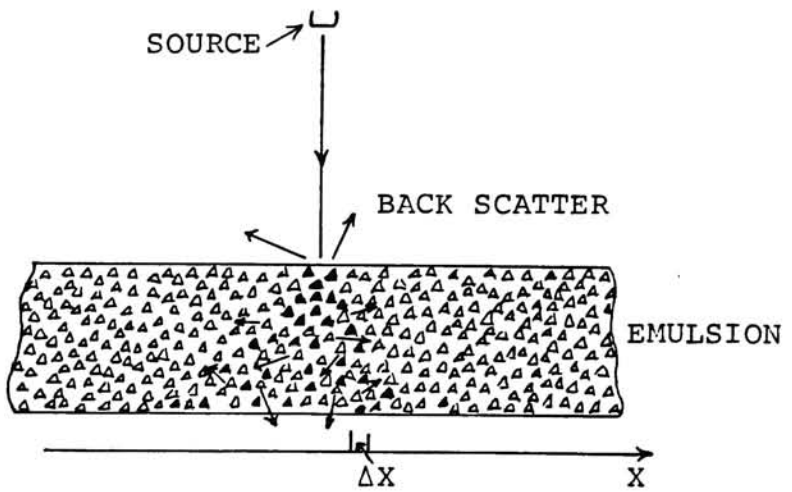

Figure 1. Cross section of emulsion during exposure. Both absorbed and scattered light are illustrated.

along the film and summing all the exposed grains above the interval Δx, a curve could be obtained showing the emulsion's reproduction of the point of light. This operation, in effect, is performed by a microdensitometer equipped with a small circular aperture. By scanning the image of a point, a trace is obtained of the illuminance distribution of the image, and is called the point spread function of the film. A second

scan would be necessary in a two dimensional distribution. Because we are dealing with symmetric distributions, a rectangular aperture is used, and only a single scan needed. The result is called the line spread function, and is defined as the illuminance distribution of the image of a line. If the PSF is denoted by $p(x,y)$, then the line spread function, $s(x)=\int_{-\infty}^{\infty} p(x,y)\,\partial y$. The point or line spread function represents the most basic form of illuminance distribution; and all other such distributions can be found by summing the spread functions from each point on the object curve. This is the reason the spread function is expressed in terms of illuminance or exposure. These quantities are additive, as opposed to transmittance, an exponential function, which would be much more difficult to apply.

It is possible to determine the image distribution, by knowing the illuminance function of the object, and the line spread function of the imageing system. The one dimensional image function, $g(x)$, is found by convoluting* the object function, $f(x)$, with the system line spread function, $s(x)$. To see how this is produced, imagine an object function, $f(x)$, divided into small elements of $f(\eta)\Delta\eta$, so that $f(x)= \Sigma f(\eta)\Delta\eta$. By making $\Delta\eta$ very small, $f(x)= \int f(\eta)\,\partial\eta$. This object is then imaged by a photo-optical system of line spread function, $s(x)$, and the resulting contribution

---

* see Appendix

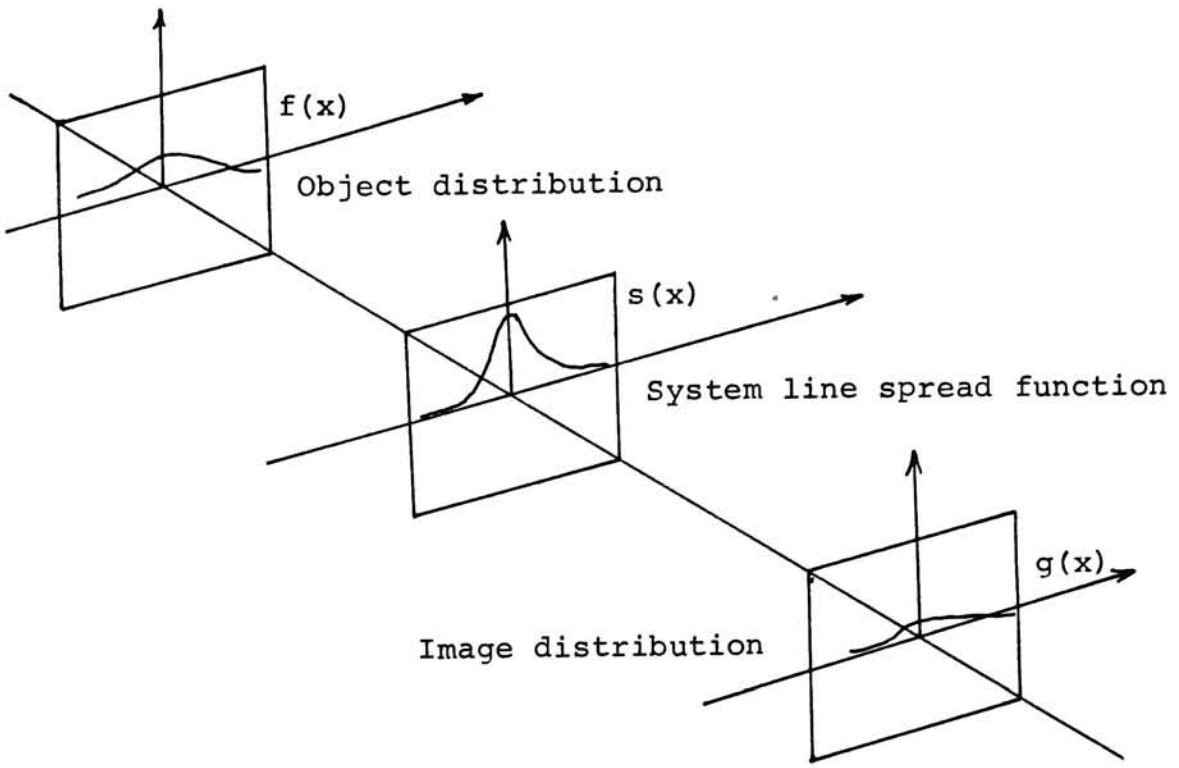

Figure 2. Image formation in photo-optical system.

of each element to the image function is $\partial g(x) = f(x-\eta)s(\eta)\partial\eta$

The total image function is $g(x) = \int f(x-\eta)s(\eta)\partial\eta$ (1)

and is shown in Figure 2. Formula (1) is called the convolution integral, and is denoted symbolically $f(x)*s(x)$. If a system contains more than one spread function, the total LSF can be found by convolution of the individual LSF's, $s(x) = s_1(x)*s_2(x)$.

Since an illuminance distribution can be found from the system LSF and the object function, then one way of evaluating a photographic system is to find the LSF representing that system. Practically, the determination of the LSF is carried out using a knife edge as object, as there is not enough energy passing through an infinitely narrow slit to expose the film sample. The effect of the edge is shown in Figure 3, beside an equivalent illustration of the theoretical function.

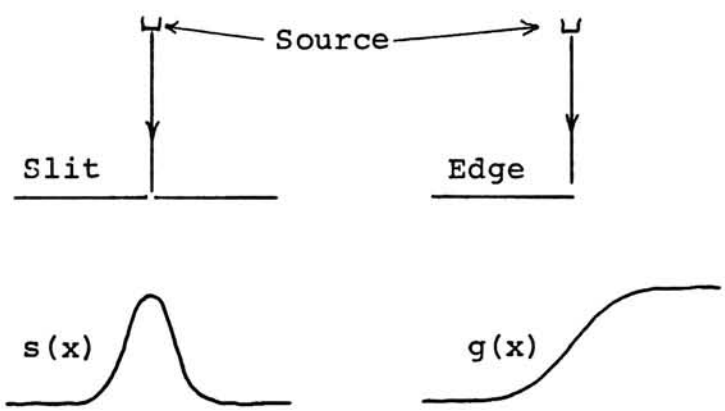

Figure 3. Determination of line spread function by slit and knife edge. LSF is the first derivative of the edge trace.

In the case of the knife edge, the object distribution is

$$f(x)=\begin{cases}1 & \text{for } x\geqslant 0\\ 0 & \text{for } x<0\,.\end{cases}$$

Let the spread function be $s(x)$. Then the illuminance function of the image is

$$g(x)= f(x)*s(x)= \int_{-\infty}^{\infty} f(\eta)\, s(x-\eta)\, \partial\eta = \int_{o}^{\infty} s(x-\eta)\, \partial\eta$$

and setting $x-\eta= \xi$

$$g(x)= \int_{-\infty}^{x} s(\xi)\, \partial\xi$$

showing that the line spread function is the first derivative of the edge trace. The edge trace method incorporates an averageing effect due to the graphical analysis, so is not overly susceptible to image noise. In contrast, by the theoretical method

$$f(x)=\begin{cases}1 & \text{for } x=0 \qquad \text{(unit impulse function)}\\ 0 & \text{elsewhere}\end{cases}$$

so $g(x)= f(x)*s(x)$, and the convolution of any function with the delta function gives that function itself. So for this instance, $g(x)= s(x)$.

We can apply the same technique to any object distribution[3]. If the object is a sinusoidal function, then

$f(x)= a_0-a\cos\omega x$ where a_0 is the D.C. level, and a is the amplitude at frequency ω. This object, reproduced by an emulsion, yields $g(x)= f(x)*s(x)$. Representing $\cos\omega x$ by the real part of the complex $e^{i\omega x}$,

$$f(x)= a_0- a\ \mathrm{Rl}\left[e^{i\omega x}\right]$$

and the image becomes

$$g(x) = f(x) * s(x) = \int_{-\infty}^{\infty} \left[a_0 - a \; Rl\left[e^{i\omega(x-\eta)} \right] \right] s(\eta)\, \partial\eta$$

$$= a_0 \int_{-\infty}^{\infty} s(\eta)\, \partial\eta - a \; Rl\left[e^{i\omega x} \int_{-\infty}^{\infty} e^{-i\omega\eta} s(\eta)\, \partial\eta \right].$$

Now $\int_{-\infty}^{\infty} s(\eta)\, \partial\eta$ is a constant= c, and

$\int_{-\infty}^{\infty} e^{-i\omega\eta} s(\eta)\, \partial\eta$

is the Fourier transform*, $F(\omega)$, of $s(\eta)$, so

$$g(x) = a_0 c - a \; Rl\left[e^{i\omega x} \; F(\omega) \right]$$

$$= a_0 c - a \; |F(\omega)| \; Rl\left[e^{i(\omega x - \phi)} \right]$$

and normalizing, $g_n(x) = g(x) \div c$

$$g_n(x) = a_0 - a \frac{|F(\omega)|}{c} \cos(\omega x - \phi).$$

In dealing with film, $s(x)$ is generally symmetrical, and $\phi = 0$

so $$g_n(x) = a_0 - a \frac{|F(\omega)|}{c} \cos \omega x. \qquad (2)$$

Comparing this to the object, the D.C. level has not changed, but the variation in amplitude is now influenced by a factor dependent on the frequency of oscillation. The effect is illustrated in Figure 4.

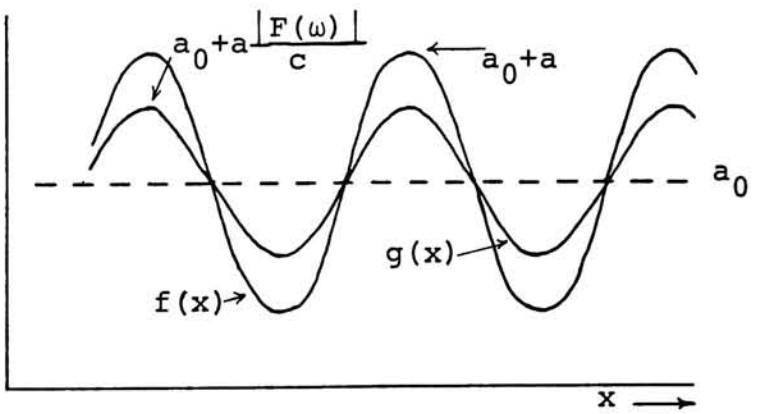

Figure 4. Comparison of image and object distributions.

---

* see Appendix

This modulation factor forms the basis for all further discussion. In curves such as the one above, it shows the relationship between maximum or minimum amplitude, and the D.C. level. In f(x), the object distribution, modulation= a/a_0, and in g(x), the image distribution, $M_i = \frac{a\,|F(\omega)|/c}{a_0}$. To see how well the output distribution represents the input, the two modulations are compared, and the result called the modulation transfer, $M_i/M_o = \frac{|F(\omega)|}{c}$. This is in the case where the spread function is symmetrical, and normalization has occurred. The modulation transfer function is the Fourier transform of the line spread function of the photo-optical system. This transform has bridged level 1 and 2 in our four level image quality scheme.

If the curves f(x) and g(x) are known, as from micro-densitometer traces, MTF can be determined directly from the maxima and minima of these curves. For any frequency,

$$MTF = \frac{g_{max}-g_{min}}{g_{max}\ g_{min}} \Big/ \frac{f_{max}-f_{min}}{f_{max}\ f_{min}}.$$

Continued over the desired frequency range, a curve is produced, representing the frequency response of the system. This is the method used in this experiment to determine MTF.

The formulas above were derived from sinusoidal input functions. If the object is other than sinusoidal, Fourier analysis must be used to first split the object and image into their sinusoidal components. Input and output modulations are found by summing the modulations of the corresponding harmonics. Then $MTF = M_{image}/M_{object}$ as before.

When a system containing several elements is to be tested, this method can be used if only the overall MTF is desired. However, the MTF of a single element can be found by proceeding as follows. For a system of three parts,

$$s(x)=s_1(x)*s_2(x)*s_3(x)$$

$$\mathcal{F}[s(x)]=\mathcal{F}[s_1(x)*s_2(x)*s_3(x)]$$

so $$|F(\omega)|=|F_1(\omega)|\cdot|F_2(\omega)|\cdot|F_3(\omega)| \qquad (3)$$

therefore $$|F_1(\omega)|=|F(\omega)|/|F_2(\omega)|\cdot|F_3(\omega)|$$

and $$MTF_1=c\ MTF_{tot.}/c_1c_2c_3MTF_2MTF_3$$

where $$c=\int_{-\infty}^{\infty}s(x)\,\partial x\ .$$

Note that the Fourier method applies exactly only if the system is linear, while the convolution method always holds.

A summary of the standard techniques in determining MTF from a sinusoidal target follows. First the target itself is scanned at each frequency to give a plot of the object function. Then a photographic emulsion is exposed, and developed, to show the image of the target, and is in turn placed in the microdensitometer to trace illuminance vs. distance. An example is shown in Figure 5_a. Because development is a non-linear operation, D_{max} and D_{min} from each trace must be converted to H_{max} and H_{min}, the effective exposure values. This is done by exposing another strip of film to a photographic step tablet, and scanning the developed image in the same microdensitometer. This produces a plot of density vs. exposure, Figure 5_b. By reflecting each desired density value on this graph, equivalent values

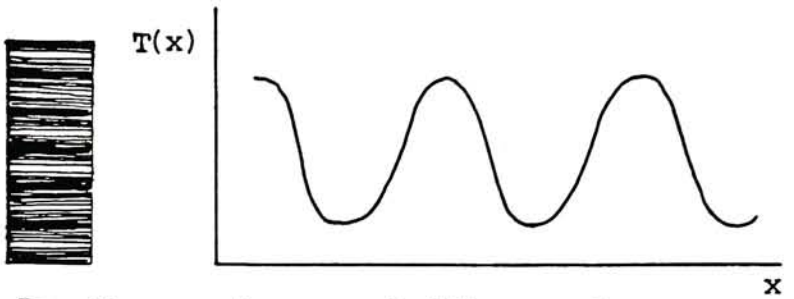

Figure 5a. Trace of exposed film sample.

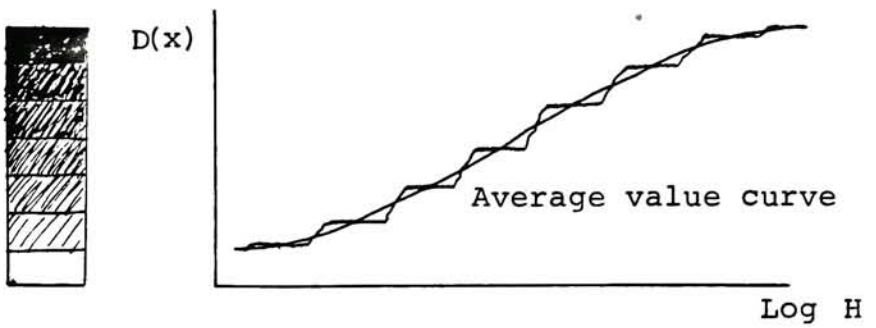

Figure 5b. Relation of transmittance to effective exposure.

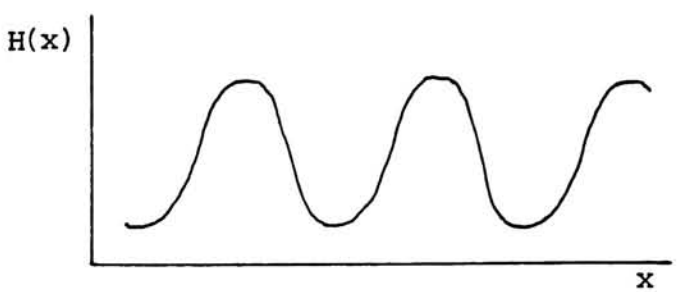

Figure 5c. Trace converted to exposure vs. distance.

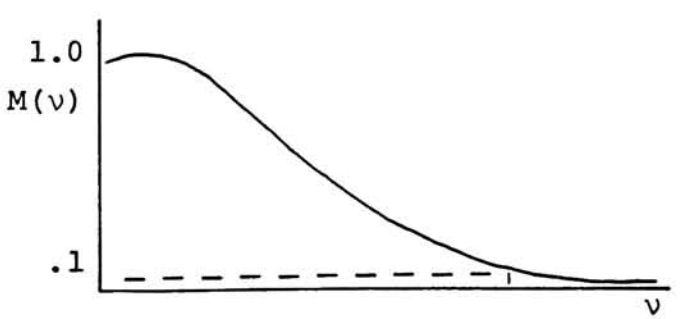

Figure 5d. MTF found from original target and exposure trace.

of exposure are obtained. If the entire trace is reflected, the curve will appear as in Figure 5_c. Usually, only the maximum and minimum values are needed, and the output modulation found from $(H_{max}-H_{min})/(H_{max}+H_{min})$ for each frequency. A sample MTF curve is drawn in Figure 5_d.

MTF gives the overall frequency response of the emulsion, but there are two areas of the function which are of particular interest. These are the shape of the curve near $\nu=0$, and the frequency at which MTF=.10. The curve shape at low frequency will indicate how well the film will reproduce edges. High MTF values in low frequencies indicate high acutance. Similarly, the higher the frequency value at the point where MTF= .1, the better the film is at reproducing fine detail. This is the resolving power of the emulsion. Both these parameters are part of the third level of image analysis.

The final stage, subjective opinion, is dependent on all the previous parameters, plus others such as graininess, and even the pictorial content of the image.

The methods described so far are useful in determining the capabilities of the photographic system as a whole, as they deal with the combined film-developer effect. Problems arise when either the input or developer is changed drastically. These problems are caused by the non-linear adjacency of developers, and will be outlined here as they affect the MTF of the film.

The strict definition of MTF deals with light scatter in the film alone, but because of the mechanism of development, the MTF will be modified to some extent. This modification will depend on the degree of adjacency effect, which itself will depend on the type of developer, amount of agitation, temperature, etc. In Figure 6 a sharp exposure gradient exists between areas A and B of a film sample. Upon processing, the developer over B exhausts faster than over A. There is some lateral developer migration between the two areas, causing an adjacency effect. Fresh developer diffuses part way into B, and exhausted developer part way into A, with the result that

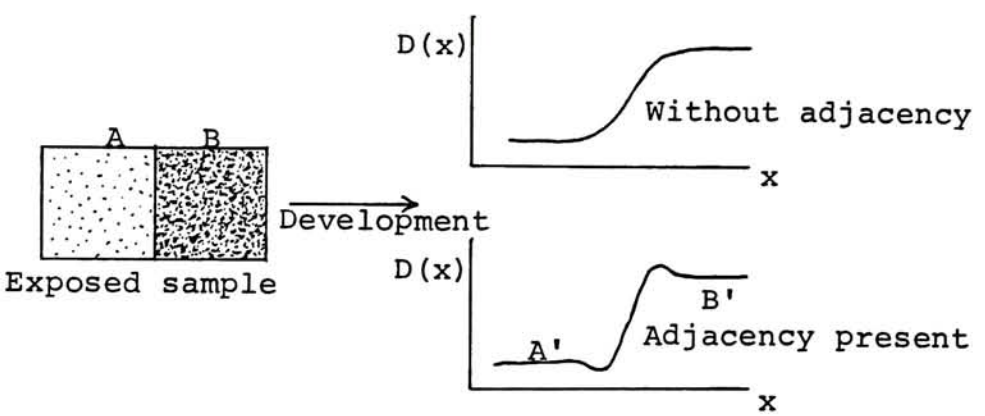

Figure 6. Effect of adjacency on trace of developed sample.

the processed film has a density distribution as in A' and B'. The apparent sharpness has increased. As a general rule, the less active the developer, the more evident the adjacency effects. More problems occur because of different

types and gradients of exposure boundaries. Figure 6 shows a knife edge exposure, but when the input is a sine wave, the extent of adjacency will not necessarily be the same. This shows that to some degree, MTF as measured here depends on the input target[4], a situation that makes predicting image distributions difficult. Different average densities will also produce different amounts of adjacency in the same type target. This has been related to the characteristic curve in a number of articles[5] [6] [7]. The problem is that the large area D log H curve used to relate trace density to effective exposure does not in general represent the true characteristic curve for the type of input used. When adjacency is present, the density difference between D_{max} and D_{min} is greater than the difference due to exposure alone. If this difference is reflected on the large area D log H curve, the apparent log H interval will in turn be greater than the actual amount. In Figure 7, the apparent density difference, when reflected on the large area curve, gives log H interval B. If this is used, calculations of the output modulation will be too large, yielding an inflated MTF. It frequently happens that MTF> 1 at low frequencies because of this. Note that in Figure 7, the less the average density of the scene, the closer the two curves are to each other, illustrating that lower average density produces less adjacency.

There are simply too many variables for the MTF of the film alone, or for MTF of inputs other than those used in

the original test, to be found from the standard method. For a generally valid prediction of a film's frequency response,

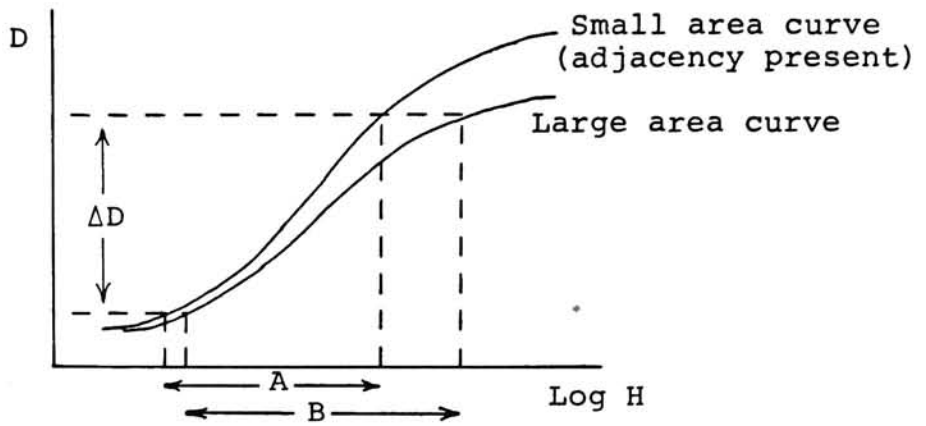

Figure 7. Effect of large area D Log H curve in converting trace densities to effective exposure. If curve B is used, the output modulation appears too large.

the Optical MTF must be used. A method devised by C.N.Nelson[5] employs mathematical means to remove the effect of the adjacency from the measured MTF. But Nelson's models are empirical, including approximations and assumptions which depend on the film-developer combination. There is no general formula at this time for mathematically predicting the effect of development. An experimental method for determining optical MTF was first described by H.Thiry[8] . The technique uses undeveloped samples in the tests, so is not susceptible to adjacency effects, and gives a result independent of the type of input. It also provides a method for direct comparison of emulsions. Finally, it can be used to monitor the effect of development, as any difference between Optical MTF and apparent MTF can be directly

related to the type of development used. In this way, Nelson's chemical spread function concept can be evaluated.

Although Thiry briefly mentions a test of a negative material, his paper deals mainly with holographic emulsions at high frequencies. The experiment is redone here to expand the results, using the same basic design to study negative films at relatively low frequencies (<200 c/mm). Suggestions for improvements to the apparatus are made in the conclusion of the thesis.

THEORY

In the study of modulation transfer functions, some sort of sinusoidal object is normally used, but here instead of the target being permanent, it is set up optically by interference. The fringe pattern is imaged directly through a microscope onto a radiometer. The trace on a chart recorder shows the object or image pattern, depending on whether a film is in place in the sample plane. A brief discussion of interference theory will be included before describing the exact experimental set-up.

By the principle of superposition, when two waves cross, the resultant displacement at any point is the sum of the displacements due to each wave separately. This can be seen for water waves simply by tossing two stones into a pool, such that the disturbance set up by one will cross the other. Both sets of waves have their own amplitude, frequency, and phase, dependent on the parameters of the source. Phase can be interpreted as that fraction of a complete vibration attained at a particular time. It will vary from point to point depending on x, the distance along the wave. When x changes by a wavelength, the phase will be the same as its starting value. The constant k, called the wave number, represents the proportion between the phase

and the displacement along the wave. The phase difference between two points x_2 and x_1 on the wave, at the same time, is δ, where $\delta=k(x_2-x_1)$.

So far we have spoken of unrelated waves, but now if it is required that both waves have the same frequency, and that the sources vary in phase by a constant, an interference effect is produced. If the origins differ by a phase ϕ, the phase difference at point P will be $\delta=k(x_2-x_1)-\phi$. Water waves from two oscillating sources of the same frequency can be studied easily, and δ calculated at any point, since ϕ is determinable, and constant.

The same general terms apply in theory to light. The light paths from two different sources can be made to superpose. But light is emitted as a burst of waves lasting about 10^{-9} seconds, each packet with random phase. So ϕ changes each 10^{-9} seconds. Interference occurs, but its pattern and position changes each time ϕ changes. The recorded result is just the average of all these interferences, or simply a steady state irradiance. For measurement of light interference, there must be some conditions established for the sources.[9]

1. Coherent sources are needed. All apparent sources must emit light of the same, or proportional phase*. Inthis way, even though the phase shifts randomly every 10^{-9} seconds,

---

* In the set-up used here, apparent sources are 180 degrees out of phase, but this relationship continually exists.

it does so the same for each source, so the effects cancel. Such sources may be devised by using a source and its optical image, or by using two images of the same source.

2. The amplitude of the two apparent sources must be roughly the same, otherwise the difference between maxima and minima in the interference pattern will be small, if not measureless.

3. The optical path difference should not be too great. Due to the finite speed of light, the beginning of one burst of light leads the other by approximately 30 cm. The illustration in Figure 8 represents the parts of two waves which will interfere in a stationary location. Between source 2 and 2_i,

SOURCE 1 {PHASE A_1} {PHASE B_1} {PHASE C_1}

SOURCE 2i {PHASE A_{2i}} {PHASE B_{2i}} {PHASE C_{2i}}

2ii {PHASE A_{2ii}} {PHASE B_{2ii}} {PHASE C_{2ii}}

2iii {PHASE A_{2iii}}{PHASE B_{2iii}}

Figure 8. Graphical representation of phase difference between source 1 and 2. Phase A1 and A2 must overlap for interference to be detected. Source 1 and 2iii will not interfere locally.

the path difference is zero, and maximum interference will occur. Source 2_{ii} will partially interfere, and source 2_{iii} will not interfere locally with source 1, since the phase difference B-A will differ from C-B, and the situation will be similar to that of incoherent sources.

The discussion to this point has dealt with sources of infinitesimal spectral width. For real sources, a second

type of coherence restriction, temporal coherence, is placed on the system, and is related to the spectral width of the source. As the spectral width, $\Delta\lambda$, increases, the visibility of interference approaches zero in only a few fringe widths. In terms of coherence length Δl, the distance from the maximum interference to the point where the visibility reaches zero, $\Delta l = \bar{\lambda}^2/\Delta\lambda$*. As an example, for white light $\bar{\lambda}$=55 Å, $\Delta\lambda$=30 Å, so $\Delta l \simeq 100$ Å. Since the average wavelength is approximately 50 Å, this means there will be two fringes visible. This concept of visibility will be further discussed later.

To summarize: A single source is devided by wavefront or amplitude to produce two waves of the same frequency which then travel along different optical paths, and are then made to intersect. Interference is the study of the superposition of these two waves.

---

* From the wave uncertainty relation for the propagation of wave packets;[10] $\Delta t \Delta\nu \geq \frac{1}{4\pi} \simeq 1$, where Δt, the coherence time, is the average duration of wave trains of a light disturbance, and $\Delta\nu$ is the effective frequency range of the Fourier spectrum of the disturbance. Now $\nu = c/\lambda$ so $\Delta\nu = c\Delta\lambda/\bar{\lambda}^2$. Also $\Delta l = c\Delta t$, so $\Delta l = \bar{\lambda}^2/\Delta\lambda$, where Δl is the coherence length.

In studying interference, a wave of the form $\Psi=Ae^{i(kx-\omega t)}$ will be used, and is shown here to satisfy the general wave equation $\partial^2\Psi(x,t)/\partial x^2= (1/v^2)\partial^2\Psi(x,t)/\partial t^2$. This equation determines the properties of motion of a wave travelling along the x-axis, and has a general solution $\Psi= f(x\pm vt)$. Taking the complex solution of a transverse wave, the real part of $Ae^{i(kx-\omega t)}$ will be shown to satisfy the wave equation.

$$\Psi(x,t)= Ae^{i(kx-\omega t)}$$

$$\frac{\partial^2\Psi}{\partial x^2} = Ak\, e^{i(kx-\omega t)}= k^2\Psi(x,t)$$

Similarly $\partial^2\Psi/\partial t^2= \omega^2\Psi(x,t)$

Now $\omega^2\Psi(x,t)/k^2\Psi(x,t)= \omega^2/k^2= v^2$

So $\partial^2\Psi(x,t)/\partial x^2= (1/v^2)\partial^2\Psi(x,t)/\partial t^2$

showing $\Psi(x,t)= Ae^{i(kx-\omega t)}$ is a valid solution. Furthermore, if the wave travels through a series of mediums, then $\Psi(x,t)= Ae^{i(-\omega t+\Sigma k_i x_i)}$, where k_i changes in proportion to the velocity of the wave in the medium. The quantity $\sum k_i x_i$ represents the phase ϕ, so the equation may be rewritten $\Psi(x,t)= Ae^{i(-\omega t+\phi)}$. When two waves are made to superpose, the total effect is

$$\Psi(x,t)= A_1e^{i(-\omega t+\phi_1)}+A_2e^{i(-\omega t+\phi_2)}$$

or $Ae^{i\phi}= A_1e^{i\phi_1}+A_2e^{i\phi_2}$.

It is useful to determine time average power of the wave $Ae^{i\phi}$, since this indicates the irradiance, which can be measured by a radiometer.

Since

$$\langle P(t)\rangle = (Ae^{i\phi})(Ae^{-i\phi})= (A_1e^{i\phi_1}+A_2e^{i\phi_2})(A_1e^{-i\phi_1}+A_2e^{-i\phi_2})$$

setting $E=A^2$

$$E=E_1+E_2+2\sqrt{E_1E_2}\cos\delta$$

where δ is the phase difference. The total irradiance is the sum of the two waves plus a modifying term dependent on the phase difference between the waves. This is responsible for the interference, containing a harmonic term $\cos\delta$, and a modulation factor. When dealing with light, it is optical path difference which is measured. Instead of ϕ, we use k_ix_i and for the case where each path is through a single medium, $\phi=kx$, $\delta=k(x_2-x_1)=k\Delta s$. The optical path difference, Δs, is a variable which increases as the point under observation moves away from the central position, producing the fringes in the interference pattern. The general equation now becomes $$E=(E_1+E_2)\left[1+(2\sqrt{E_1E_2})/(E_1+E_2)\cos\frac{2\pi\Delta s}{\lambda}\right] \quad (4)$$

where $k=\frac{2\pi}{\lambda}$.

Thomas Young was the first to produce interference effects using division of wavefront. This is a valuable experiment to study, as many other designs are quite similar to it, and only slight mathematical changes are required to derive equivalent parameters. In Young's set up, monochromatic light from a primary point source is intercepted by a plate with two holes whose size and separation is small (the diameter of each aperature is of the order of the wavelength of light). An image screen is placed a distance R from the secondary sources, parallel to the object plane, such that R>>D. Waves leave 1 and 2 in phase (both apertures are

equidistant from the primary source), and intersect at P. The difference in their optical paths is $s_2-s_1=\Delta s$. We wish to determine this quantity to predict the appearance of the interference pattern on the image screen.

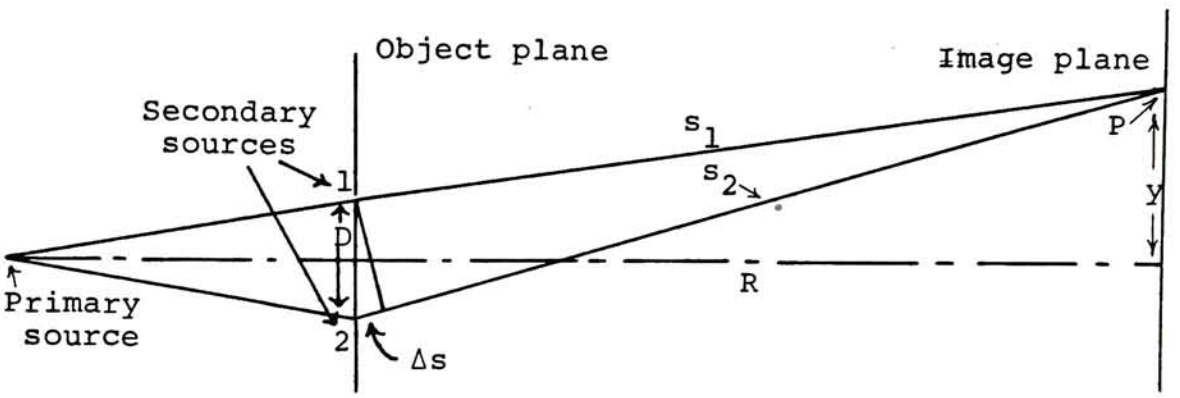

Figure 9. Young's experiment. Interference between sources 1 and 2 is observed on the image plane at point P.

In Figure 9, at any point P,

$$s_2^2=(y+\frac{D}{2})^2+R^2 \quad \text{and} \quad s_1^2=(y-\frac{D}{2})^2+R^2$$

$$s_2^2-s_1^2=2yD$$

so $$s_2-s_1=\Delta s\ \frac{2yD}{s_2+s_1}$$ and since $R>>D$, $2R\approx s_2+s_1$

giving $$\Delta s=\frac{yD}{R}.$$

The irradiance at point P is now

$$E=(E_1+E_2)\left[1+\frac{2\sqrt{E_1E_2}}{E_1+E_2}\cos\ 2\pi y\frac{D}{\lambda R}\right] \qquad (5)$$

where the period of the disturbance is $\frac{\lambda R}{D}$. The maximum value of this function occurs when $\cos\ \frac{2\pi}{\lambda}\ \frac{yD}{R}=1$, and the minimum when $\cos\ \frac{2\pi}{\lambda}\ \frac{yD}{R}=-1$. That is

when $\frac{yD}{R}=m$ $\quad m=0,1,2,3,\ldots$ there is a maximum

or $$y=\frac{mR}{D},$$

and when $\frac{yD}{R} = m+\frac{1}{2}$ $\quad m=0,1,2,3,\ldots$

or $\quad y=(m+\frac{1}{2})\frac{\lambda R}{D}$

there is a minimum. The integer m is the order of interference, and the fringes called the zero, first, second, and third orders respectively.

The irradiance distribution in the image plane of a monochromatic source is shown in Figure 10. With the secondary sources in phase, the pattern has a maximum at x=0, the perpendicular bisector of the line connecting the sources. Secondary sources out of phase cause the curve to shift laterally by an amount proportional to the phase difference. If this difference is π radians, the pattern at x=0 will have minimum irradiance.

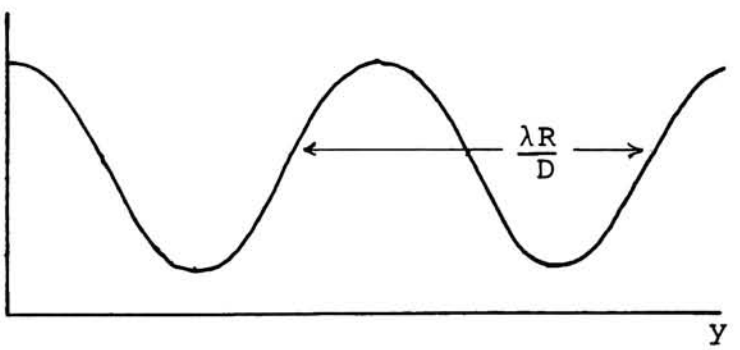

Figure 10. Shape of fringes resulting from interference of monochromatic sources.

Spatial frequency depends on the distance between the secondary sources, the distance between the source and image planes, and the wavelength of the illumination. If no change is made in the structure of the apparatus, it can be seen

from the formula, fringe separation $=\frac{R}{D}$, that the period of the interference pattern is directly proportional to the wavelength of the source. If the light consists of two emitted wavelengths, the contributions are mutually incoherent, and the total distribution is just the sum of each function individually, as in Figure 11. The coherence length is very short in this case, with the visibility reaching zero after only one period. For a real source of spectral width $\Delta\lambda$, there is a distinctive envelope on the pattern as in Figure 12, which can be predicted if the spectral distribution of the source is known.[10]

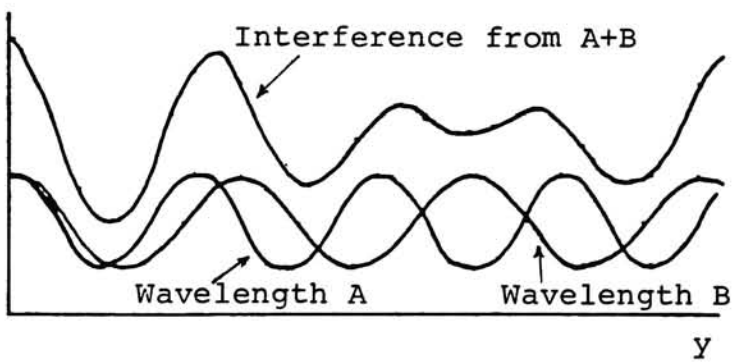

Figure 11. Interference due to primary source of two emitted wavelengths is the sum of each pattern separately.

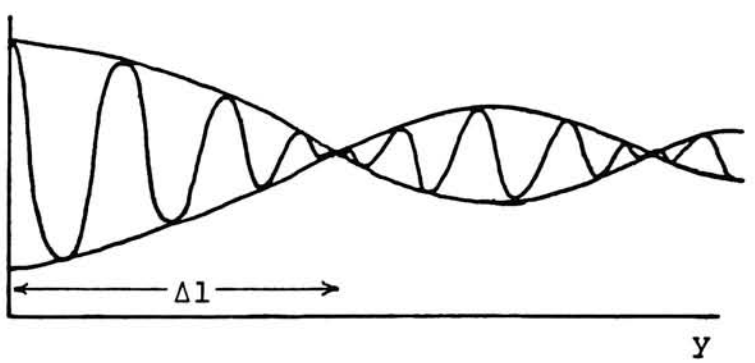

Figure 12. Interference pattern of source of bandwidth $\Delta\lambda$. Coherence length decreases as $\Delta\lambda$ increases.

To determine the envelope, or visibility curve, the light source is regarded as a summation of monochromatic sources over the spectral width $\Delta\lambda$. The irradiance of each element over the wave number range ∂k_0 may be calculated by equation 5 as

$$e_0(k_0,\Delta s)=2e_1(k_0)\left[1+\cos\ k_0\Delta s\right]\partial k_0 \qquad (6)$$

where $k_0=2\pi/\lambda_0$, optical path difference $\Delta s=\delta/k_0$, and $e_1(k_0)$ is the spectral irradiance distribution of the section of the beam at k_0. (Both beams will have the same irradiance for the purpose of this discussion). All spectral components add incoherently, and the total irradiance is

$$E(\Delta s)=2\int e_1(k_0)\left[1+\cos\ k_0\Delta s\right]\partial k_0 .$$

If $\bar{k}_0$ is the central position of the source, let x be such that $k_0=\bar{k}_0+x$; then the irradiance in the interval ∂k_0 is

$$j(x)=e_1(\bar{k}_0+x).$$

Now
$$E=2\int j(x)\left[1+\cos\left((\bar{k}_0+x)\Delta s\right)\right]\partial x$$
$$=P+\cos\ \bar{k}_0\Delta s\ C(\Delta s)-\sin\ \bar{k}_0\Delta s\ S(\Delta s)$$
$$=P+\sqrt{C^2+S^2}\left[\frac{C\cos\ \bar{k}_0\Delta s}{\sqrt{C^2+S^2}}-\frac{S\sin\ \bar{k}_0\Delta s}{\sqrt{C^2+S^2}}\right]$$

where
$$P=2\int j(x)\,\partial x$$
$$C=2\int j(x)\ \cos\ x\Delta s\ \partial x$$
$$S=2\int j(x)\ \sin\ x\Delta s\ \partial x .$$

From Figure 13, with tan =S/C

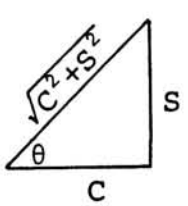

Figure 13. Relation of parameters S and C.

$$E=P+\sqrt{C^2+S^2}\ (\cos\theta\ \cos\ \bar{k}_0\Delta s-\sin\theta\ \sin\ \bar{k}_0\Delta s)$$

which may also be written

$$E=P\left[1+\frac{\sqrt{C^2+S^2}}{P}\cos\ \bar{k}_0\Delta s+\theta\right]. \qquad (7)$$

For the normalized distribution, E/P, the visibility

$$(E_{max}-E_{min})/(E_{max}+E_{min})=\sqrt{C^2+S^2}/P=V\ .$$

This procedure is equivalent to taking the Fourier transform of the spectral distribution, going to Δs space instead of ω space. C and S are the Fourier cosine and sine transforms of the function j(x). $\sqrt{C^2+S^2}$ is $\left|F(\Delta S)\right|$ and in complex form

$$\left|F(\Delta S)\right|=\int j(x)e^{-i\Delta sx}\partial x. \qquad (8)$$

P is the normalization factor. An equivalent expression was used in the introduction to show that MTF is the Fourier transform of the spread function. Here MTF is replaced by the visibility envelope $V(\Delta s)$, and the spread function by the spectral distribution.

For a spectral distribution of gaussian shape,

$$j(x)=j_0e^{-a^2x^2} \qquad a=\sqrt{2\ln 2}/\Delta k\ .$$

Visibility $V(\Delta s)=\int j(x)e^{-i\Delta sx}\partial x$

$$=j_0e^{-\Delta s^2/(4a^2)}\int e^{-(ax+\frac{i\Delta s}{2a})^2}\partial x\ .$$

Setting $y=ax+\frac{i\Delta s}{2a}$, $\partial y=a\partial x$,

$$V(\Delta s)=\frac{1}{a}\ e^{-\Delta s^2/(4a^2)}\int e^{-y^2}\partial y$$

$$=j_0\sqrt{\pi}/a\ e^{-\Delta s^2/4a^2}=1 \text{ at } \Delta s=0 \text{ in the}$$

normalized function, so

$$V_n(\Delta s)=\ e^{-(\Delta s/2a)^2}.$$

This is the type of visibility function resulting from the spectral distribution of a Helium-Neon laser, Figure 14. In

this case, the optical path difference Δs, has a value of 4.5 cm when $V(\Delta s)=.1$. To that point, 71000 wavelengths can be observed.

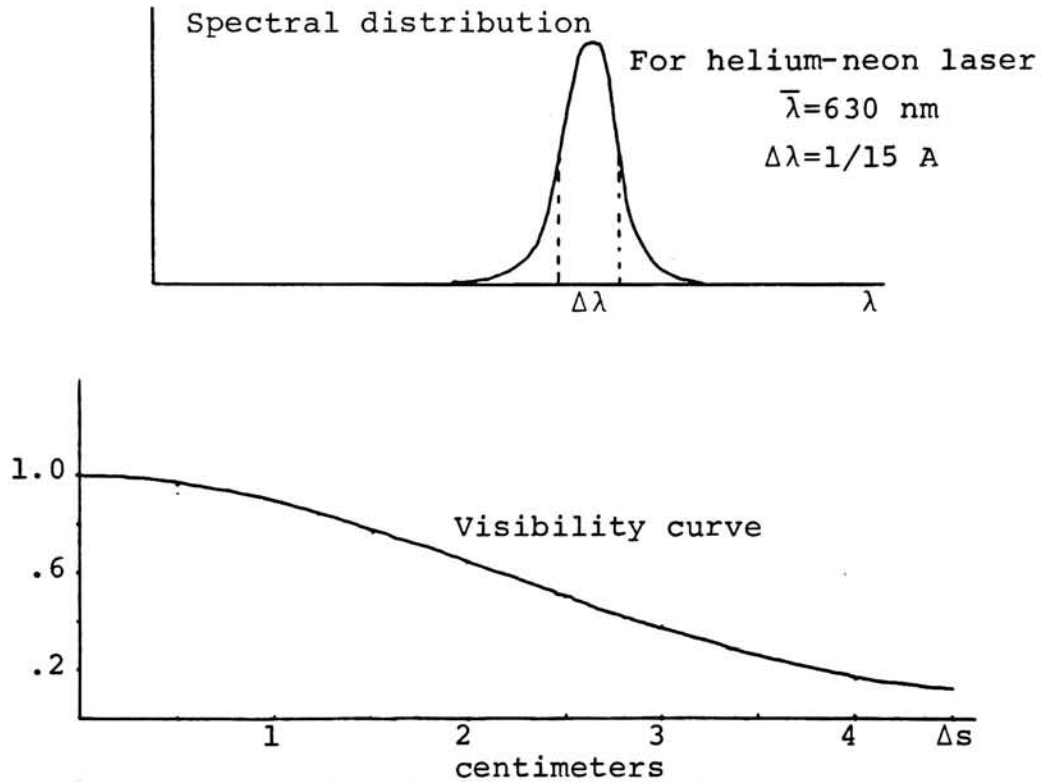

Figure 14. Spectral distribution and visibility curves for Helium-Neon laser.

The Lloyd's mirror arrangement in Figure 15 consists of a primary source placed a distance from an optical flat, such that light from it hits the mirror at near grazing incidence. The image plane is located perpendicular to the mirror. A point P located on this plane receives light directly from source 1, and from its virtual image at 2. Interference will occur at P just as in Young's experiment, with only a few differences. First, the virtual source is a reflected image

of the real source, and this results in a phase difference of π between the sources, giving an irradiance minimum at the zero order fringe. Second, interference can only occur when both sources are visible to the point on the image plane.

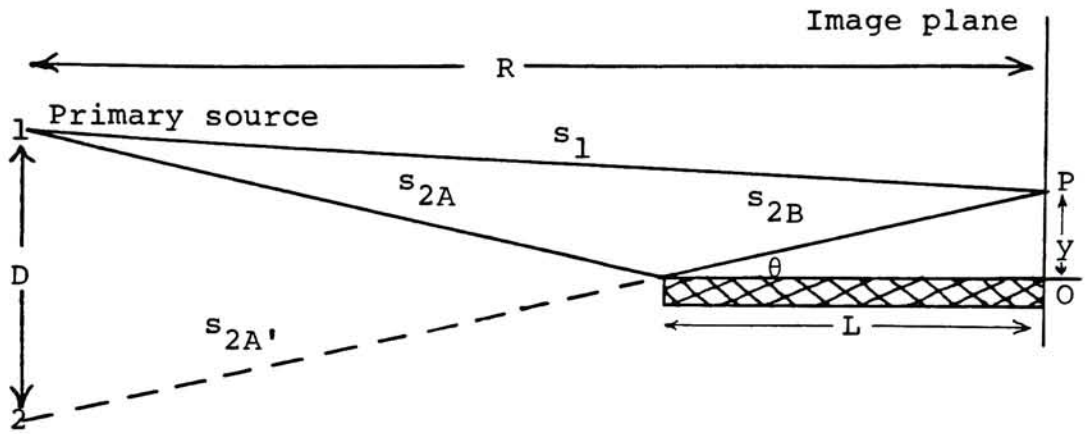

Figure 15. Lloyd's mirror. Interference occurs between primary source and its virtual image.

When the light reaching P comes from the front edge of the mirror, the maximum extent of interference has been reached; that is, θ can get no larger unless changes are made to the apparatus. Third, the irradiance of the two sources can never be identical, since reflectance is at least slightly less than 100%. E_{min} on the interference pattern therefore never reaches zero. This is certainly not a drawback since radiometer error increases as irradiance approaches zero.

One of the great advantages of the Lloyd's mirror set-up is the ease with which spatial frequency of the pattern is changed. From Young's experiment, fringe separation=$\lambda R/D$. Here, R/D is approximately $1/2\sin\theta$, so for

Lloyd's mirror, fringe separation=$\lambda/2\sin\theta=\lambda/2\theta$ for small θ. As θ increases, fringe separation decreases, so simply by rotating the mirror and image plane together about their intersection, the spatial frequency of the irradiance distribution is changed.

EXPERIMENTAL

The design of this experiment is formed of two parts; an image-forming or interference section, and an image-receiving or analysis area. The layout of the apparatus is shown in Figure 16.

The image-forming section includes a Helium-Neon laser, made to act as a point source by directing the beam through a negative lens. A mirror mounted on a rotating table then forms sinusoidal fringes at the sample plane. If no film is in place, the fringes represent the input. With a film at the sample plane, an output function will result. In either case the receiving apparatus is the same.

A microscope focused on the sample plane enlarges the fringes and projects the image through a slit onto a photomultiplier tube. This entire analysis section is mounted on an x-y moveable platform to allow scanning of the fringe pattern.

Recalling the theory of Lloyd's mirror, to change the frequency of the disturbance, all that is required is that the angle of the optical flat change, thus changing the angle of intersection of the two paths of light at a given point on the sample plane. At each angle, an Input and Output modulation is determined for a given set of films. Values

are obtained at specified spatial frequencies between 13 c/mm and 225 c/mm. Eight such sets are made to give sufficient statistical validity to the evaluation. By mounting a ruler over the radiometer slit, but still within the projected image of the fringes, the spatial frequency can be approximately noted, so that for subsequent sets, the same frequencies can be used.

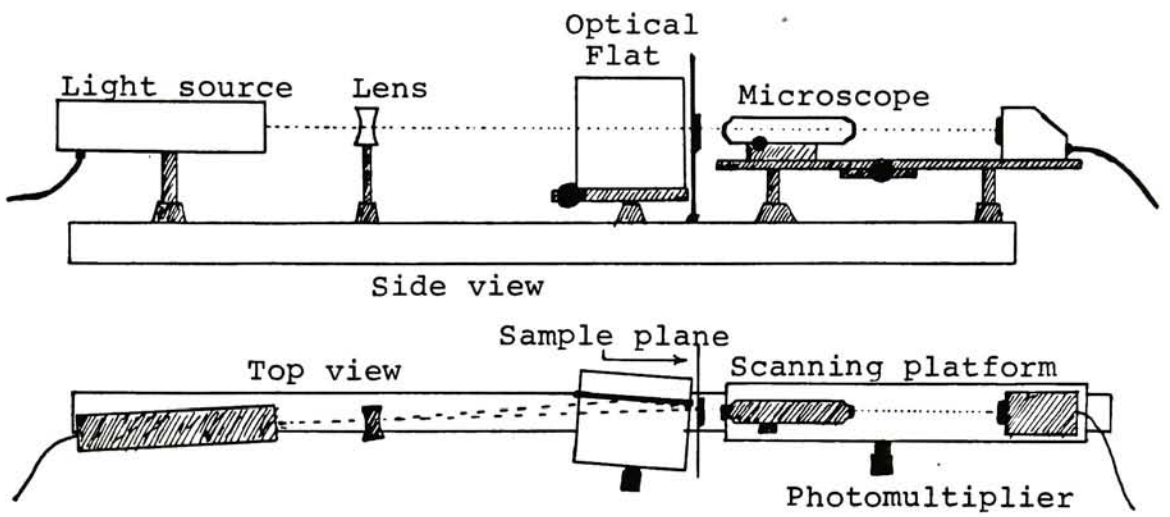

Figure 16. Lay out of experimental apparatus. Photomultiplier feeds information to radiometer (not shown).

Equipment

Light Source. A Helium-Neon laser from University Labratories (model L261) is used. This produces red light at 630 nm, and gives an output at that wavelength of approximately 3 mW. It provides the monochromatic light needed to obtain interference of high coherence length, insuring that the pattern closely resembles a sinusoidal distribution over several periods. The light is also sufficiently intense

to be recorded by the radiometer without excessive amplification, thereby minimizing instrument noise.

There would be a problem in using the laser alone, since the gaussian intensity distribution of its narrow beam would create a pronounced envelope on the interference fringes. By placing a negative lens in the incident beam, the gaussian distribution is widened, making the fringe envelope much flatter. The lens used has a focal length of -155 mm, and a diameter of 35 mm.

Optical Flat. The mirror used in this study must be optically flat, otherwise the fringes formed on the sample plane will not be straight, and vary from the calculated spatial frequency. The mirror must also allow a sufficient number of fringes to be produced for the pattern to approximate a sine wave. This sets a lower limit on obtainable frequencies, and is calculated by the following considerations*.

If the interference pattern is to represent a cosine wave, then its Fourier transform must approximate two delta functions, one located on each side of the origin at a distance $1/\tau$, where τ=wavelength of the cosine wave. Now the mirror acts as a window. Its Fourier transform is a sinc function, and represents the energy spread of the fringes. The wider the window, the narrower the sinc function, and the closer its approximation to a delta function. Too narrow

---

* A complete analysis is given in the appendix

a window will cause the interference pattern to be distorted in the lower frequencies. The minimum acceptable spatial frequency, ν_0, is determined by comparing the graph of the combined sinc functions for different small values of ν with the Fourier transform of a cosine function. As ν decreases, the width of the function increases. From Figure 17, 5 or 6 cycles will produce an adequate cosine wave. The mirror used here has a length of 200 mm, which will produce 6 or more cycles down to about 10 c/mm. In this experiment, a minimum of 13 c/mm is used.

To change the spatial frequency of the fringes the mirror is simply rotated and positioned in the proper lateral location using a micrometer with an x-y mount. The lateral location is changed each time the mirror is rotated to insure that the same portion of the incident light beam is used in each case. Again, this is necessary because of the gaussian intensity distribution of the light.

Although the reflectance of the mirror should be high so that both sources have about the same apparent irradiance, it is important that it not be too close to 100%, as then the minimum value on the traces would approach zero for input modulation, causing excessive instrument noise. This mirror exhibits an 85% reflentance, found to be quite acceptable.

Sample Plane. The film holder consists of a thin blackened metal plate in which a small hole is cut to allow the

passage of light. Film samples are attached over this window. This is a simple method, but quite convenient, as changing samples can be performed quickly and easily.

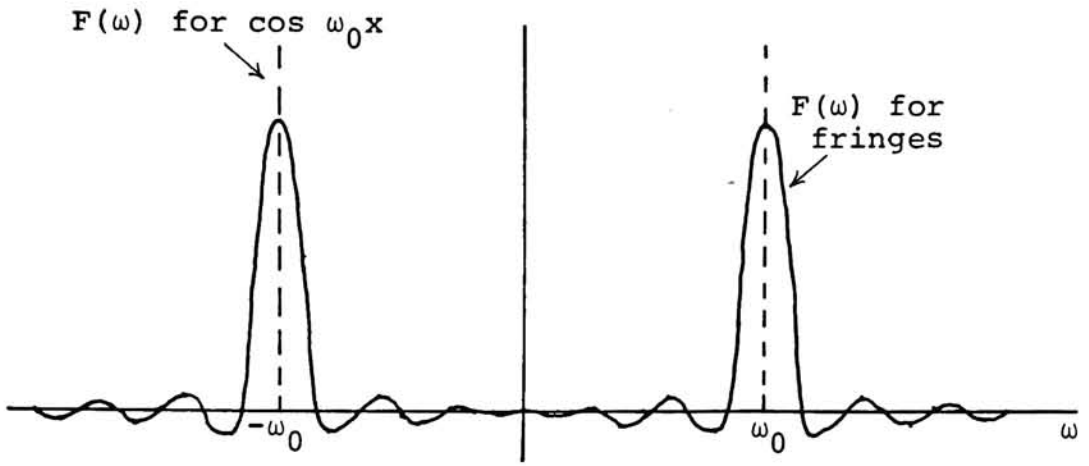

Figure 17. Fourier transform of interference fringes with frequency of 10 c/mm. Six cycles are visible along the image plane.

Image Analysis Section. The microscope is a Rolyn Arcadia, with a 215 mm, .40 NA, 20 X Bausch & Lomb objective, and a 5X eyepiece. It is focused at that location where, with the film sample in place, irradiance variation is at its maximum. This setting is then maintained throughout the tests.

In this study, the microscope acts as a projector, directing the image onto the slit of the photomultiplier at a magnification of 65.6 times. The entire microscope-photomultiplier system is set on a moveable stage, whose

lateral adjustment enables the slit to scan the fringes at the film plane.

A photomultiplier tube, General Electric Model 931a integrates the irradiance on the slit and displays the result on a Microphotometer (Aminco Model 10-213). The entrance slit is adjusted to measure 10 mm± .1 mm by .05 mm ± .0005 mm using an eyepiece calibrated by a Bausch & Lomb calibration slide. Because of the 65.6 microscope magnification, the effective slit dimensions are 152 μm x .76 μm, giving an approximate 1/200 width to length ratio.[11]

Attached to the photomultiplier is a Varian chart recorder Model G-11A. Its motor is used simultaneously to advance the graph paper onto which the pattern is traced, and to move the stage micrometer. By matching maximum irradiances with values taken from the micrometer, an accurate calculation is made of the pattern frequency.

Transmission vs. Time Test. One of the possible problems with direct scanning of film is the buildup of photolytic silver on the emulsion due to the length of exposure from the high intensity source. If this were to happen to a significant extent, the transmittance and degree of diffusion of the light would change, giving an inaccurate MTF of the sample. Different types of film were tested by aligning the laser directly on the slit of the radiometer, and placing samples in this beam. Plots of transmittance vs. time were made for Kodak Plus-X Pan 4147, Kodak High Contrast

Copy Film, Kodak Panatomic-X, GAF Versapan 2831, and Kodalith Ortho Type 3. Some of these results are shown in Figure 18. Kodak Plus-X decreased in transmittance by 16% in one minute, indicating a relatively large build-up of photolytic silver. GAF Versapan decreased 6%, also too large an amount here. But Kodak Panatomic-X, Kodak High Contrast Copy, and Kodalith Ortho Type 3 films show only a 2%, ½%, and ½% decrease after two minutes, so they were chosen for this study.

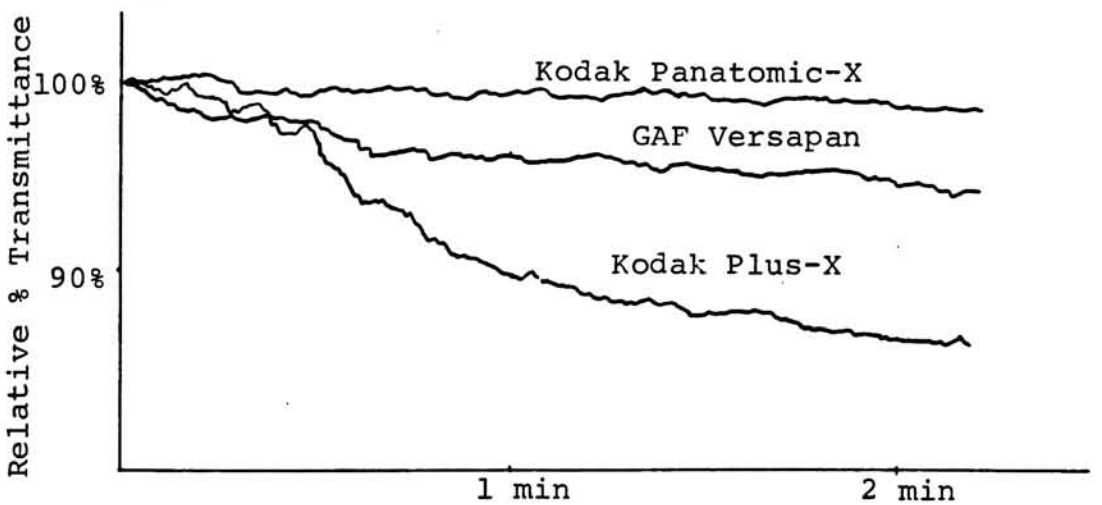

Figure 18. Transmission vs. time tests.

Since we are determining MTF due to scattered light alone, any change in the scattering properties will alter output modulation. To determine the effect of this change, I would suggest that in a separate study, the MTF of Kodak Panatomic-X be found as described here, then another sample be pre-exposed long enough to show a 7 or 8% drop in transmittance. Redetermination of MTF and comparison of the curves would illustrate the effect of print-out silver.

ANALYSIS

Using the methods described in the previous section, three films, Kodak Panatomic-X, Kodalith Ortho Type 3, and Kodak High Contrast Copy film were tested, and their calculated MTF's appear in Tables 1 to 8.

In Figure 19, the experimental results for Panatomic-X may be compared with a reference curve drawn to show MTF by the conventional method[12]. The proximity of these curves indicates that the Lloyd's mirror arrangement is feasible for at least this type of sample. Absolute values of the two curves cannot be related below 13 c/mm, since data was not obtained in that region. However, since adjacency effects tend to enhance detail in the lower frequencies, it is probable that the conventional curve has slightly higher values in that area.

Figure 20 shows the MTF for Kodalith Type 3, a lithographic film. The data is quite repeatable, and the average value curve behaves as would be expected from practical useage. No comparison curve is shown since conventional methods cannot produce a unique MTF function due to both the extremely high densities envolved (>4.0), and the strong dependence on developer activity.

The data for Kodak High Contrast Copy film, in Figure 21,

is scattered and apparently inconclusive. This variation may be explained by looking at the relation between film spread function and the type of imageing apparatus used here. With light at normal incidence, emulsion spread functions are symmetrical; but this is not strictly the case in a pattern formed by Lloyd's mirror interference. Each point on the film plane receives light from two different directions, shown in Figure 22. Furthermore, as the distance along the film increases, these angles of incidence change. This may have a drastic effect on MTF, depending on the type of spread function involved. The large k-value, corresponding to the $\frac{1}{10}$ width[13] of spread functions similar to Kodak High Contrast Copy, greatly increase the lateral diffusion of light entering from an oblique angle. This produces a significant light loss, and a deflated value of output modulation. Spread functions with smaller base widths exhibit less sideways scatter, so are less dependent on light angle. Kodak Panatomic-X, and Kodalith Ortho Type 3 films fall into this category ; so though the same angular variations of light are present as for High Contrast Copy film, the effect is not as pronounced, and the values of output modulation, and therefore MTF, are much more consistent.

There is a second factor which contributes to the angular variation of light incidence. In this arrangement, the film plane remains stationary, and does not rotate with the mirror. Ideally, the apparatus should maintain an angle

of 90^{o} between the mirror and the film plane. This dictates that each time the fringe frequency is changed, the film rotates accordingly. And the scan direction, which must be parallel to the film plane to allow precise focusing, must move through the same angle. This would involve placing the entire analysis system on a rotational micrometer of a type not available in this study.

A test has been conducted to evaluate the effects of film angle on the MTF of Kodak High Contrast Copy film between the frequencies 130 and 175 cycles/mm. This is the area showing the largest MTF variation. Fortunately, in this high frequency range, the scan direction is short enough so that the microscope need not be refocused along the scan. At each of the frequencies 130 c/mm, 140 c/mm, and 175 c/mm, the film was mounted on a rotational micrometer, and turned through a total of 10^{o}. The graphs in Figure 23 show the resulting variation. A shift of only 1^{o} from normal incidence can produce the large differences in the MTF values. These differences agree in each case with the observed fluctuations in the experimental data of Figure 21.

A curious result of the test is the fluctuation of MTF rather than a steady deterioration as the angle of film tilt was increased. This is perhaps caused by internal reflections, or by the film samples not maintaining their flatness throughout the tests. More extensive study of this fluctuation is left to future experiments.

frequency (cycles/mm)	$(E_{max}-E_{min})/(E_{max}+E_{min})$		
	Panatomic-X	Kodalith 3	High Con.
14	.89	.83	.97
20	.78	.83	.95
33	.66	.71	.90
45	.54	.59	.77
59	.41	.41	.60
81	.33	.34	.57
106	.20	.24	.70
129	.16	.13	.54
146	.17	.13	.49
170			.49
189			.57
213			.47

TABLE 1 MTF Data for test films. Run Number 1

frequency (cycles/mm)	$(E_{max}-E_{min})/(E_{max}+E_{min})$		
	Panatomic-X	Kodalith 3	High Con.
13	.88	.88	.96
20	.81	.84	.91
33	.65	.70	.80
46	.54	.61	.80
60	.42	.38	.82
84	.35	.38	.54
104	.20	.29	.53
136	.16	.12	.52
155	.18	.13	.52
171			.53
192			.51
226			.48

TABLE 2 MTF Data for test films. Run Number 2

frequency (cycles/mm)	$(E_{max}-E_{min})/(E_{max}+E_{min})$		
	Panatomic-X	Kodalith 3	High Con.
13	.88	.89	.99
20	.73	.79	.94
34	.58	.67	.88
46	.50	.59	.91
60	.44	.49	.83
80	.30	.44	.79
103	.26	.25	.48
131	.18	.15	.71
152	.17	.10	.73
170			.66
208			.45
228			.48

TABLE 3 MTF Data for test films. Run Number 3

frequency (cycles/mm)	$(E_{max}-E_{min})/(E_{max}+E_{min})$		
	Panatomic-X	Kodalith 3	High Con.
13	.88	.93	.99
20	.81	.89	.95
34	.62	.68	.95
45	.47	.58	.86
61	.41	.49	.82
82	.32	.38	.80
106	.18	.25	.56
138	.09	.16	.49
162	.09	.18	.46
179			.46
202			.44
226			.47

TABLE 4 MTF Data for test films. Run Number 4

frequency (cycles/mm)	$(E_{max}-E_{min})/(E_{max}+E_{min})$		
	Panatomic-X	Kodalith 3	High Con.
14	.92	.92	.99
21	.75	.76	.89
34	.62	.72	.88
47	.50	.50	.90
58	.35	.47	.82
83	.34	.38	.65
102	.22	.28	.69
134	.13	.19	.46
150	.05	.16	.72
164			.52
193			.48
222			.40

TABLE 5 MTF Data for test films. Run Number 5

frequency (cycles/mm)	$(E_{max}-E_{min})/(E_{max}+E_{min})$		
	Panatomic-X	Kodalith 3	High Con.
14	.90	.91	.96
20	.79	.83	.93
34	.60	.69	.94
43	.55	.59	.93
62	.43	.52	.87
78	.31	.40	.75
102	.26	.28	.51
131	.18	.21	.50
149	.12	.21	.51
172			.52
189			.51
236			.49

TABLE 6 MTF Data for test films. Run Number 6

frequency (cycles/mm)	$(E_{max}-E_{min})/(E_{max}+E_{min})$		
	Panatomic-X	Kodalith 3	High Con.
13	.88	.94	.97
19	.84	.85	.94
32	.64	.72	.91
47	.50	.58	.85
60	.40	.49	.75
76	.30	.38	.80
104	.18	.31	.52
130	.14	.22	.53
144	.14	.18	.57
175			.48
187			.50
233			.56

TABLE 7 MTF Data for test films. Run Number 7

frequency (cycles/mm)	$(E_{max}-E_{min})/(E_{max}+E_{min})$		
	Panatomic-X	Kodalith 3	High Con.
14	.86	.98	1.0
20	.79	.79	.95
29	.62	.70	.93
48	.52	.56	.90
56	.42	.48	.85
81	.32	.39	.84
103	.24	.29	.82
131	.08	.14	.67
149	.15	.13	.70
171			.51
207			.49
228			.47

TABLE 8 MTF Data for test films. Run Number 8

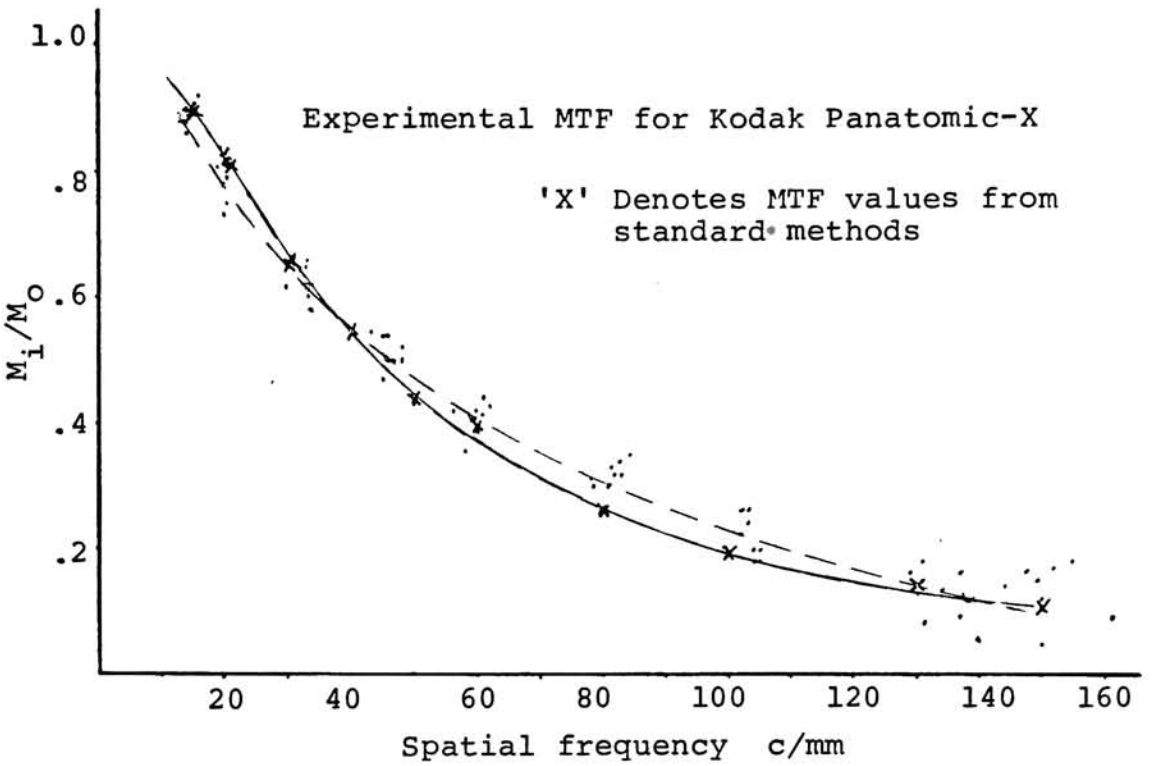

Figure 19. MTF for Kodak Panatomic-X. The solid curve shows the frequency response derived from traditional methods. The dashed curve represents the approximate average values of the data.

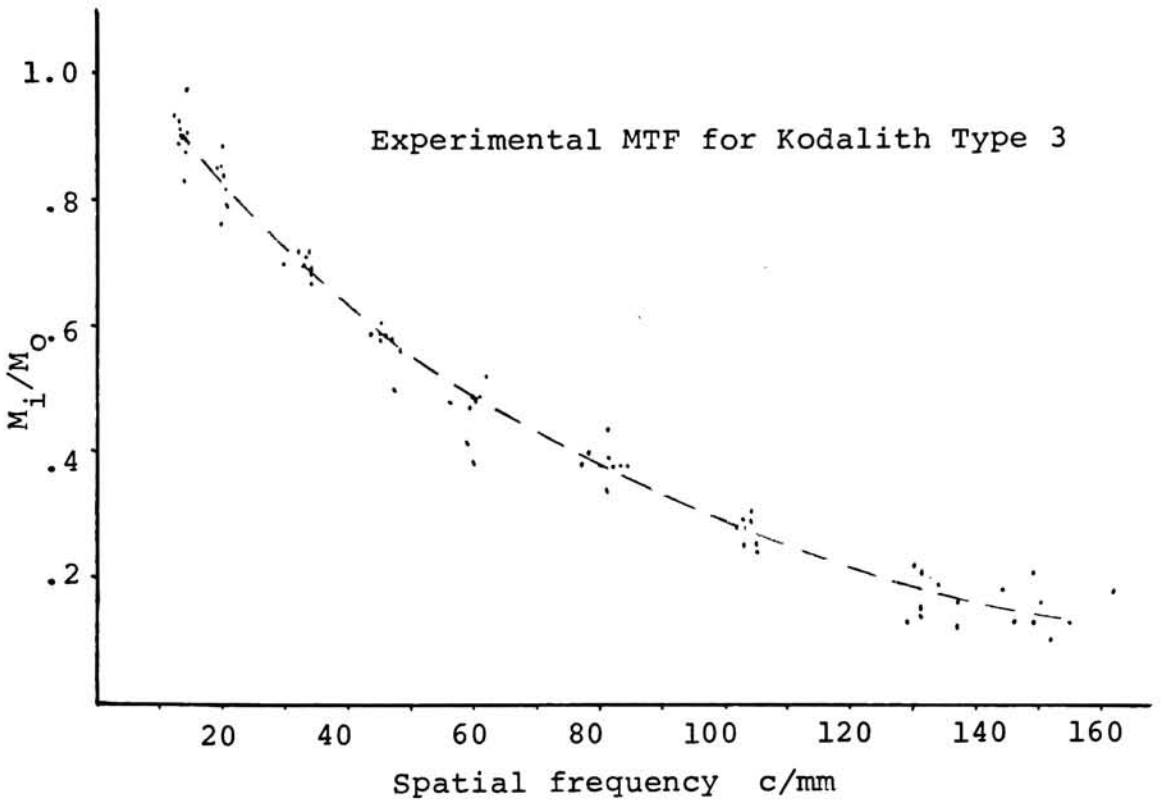

Figure 20. MTF for Kodalith Type 3. The dashed curve represents the approximate average values of the data.

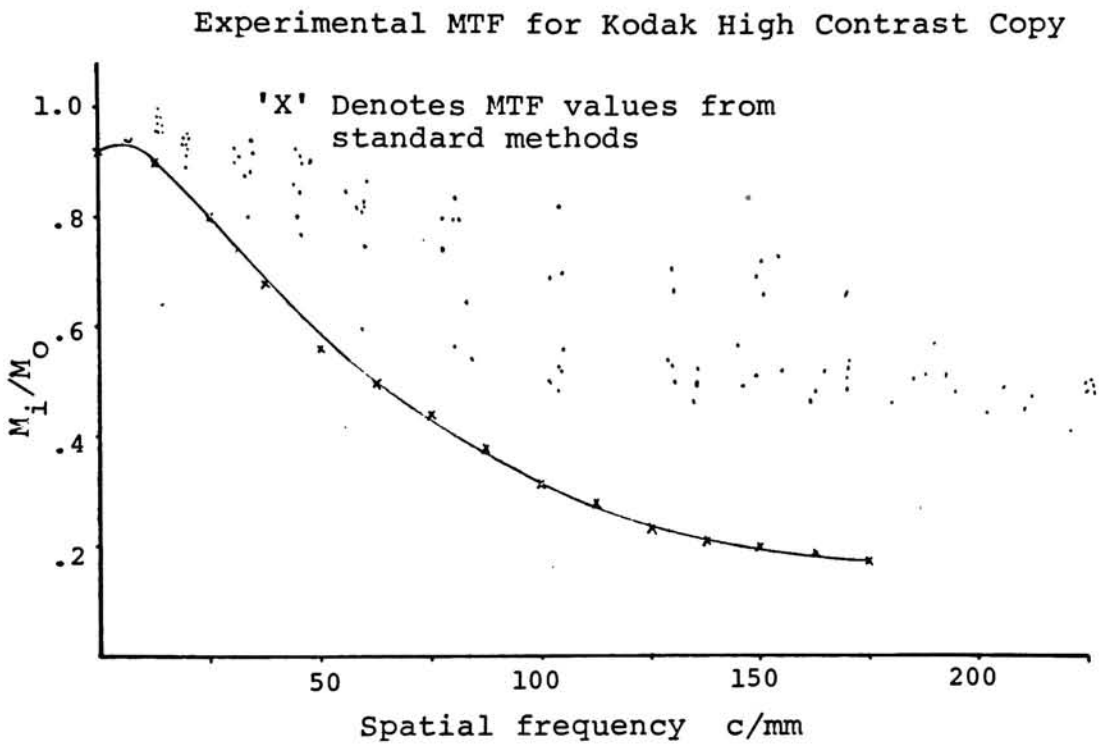

Figure 21. MTF for Kodak High Contrast Copy. The solid curve shows the frequency response derived from traditional methods. No average value curve is drawn here due to the large variability in the data.

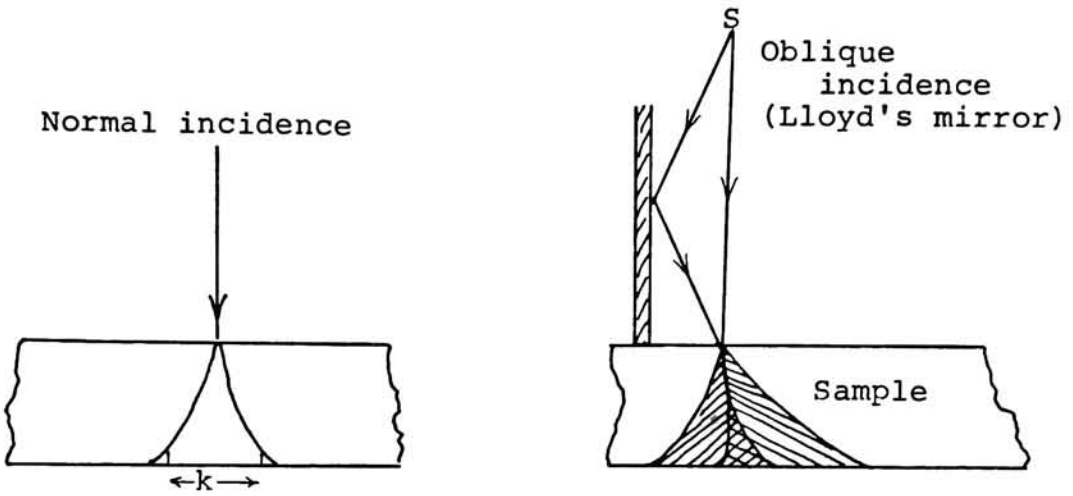

Spread function with small k-value

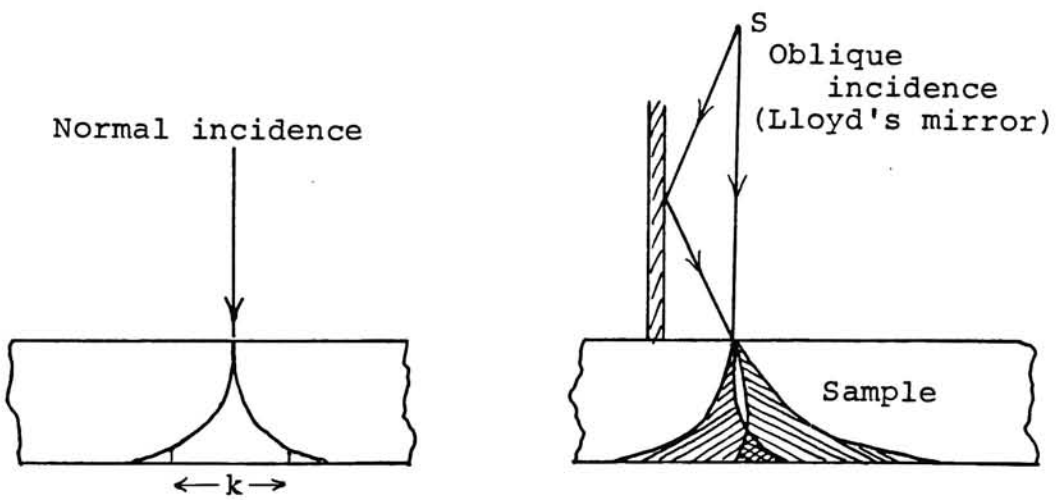

Spread function with large k-value

Figure 22. Effect of k-value of film on oblique incidence of light. The larger the k-value of the emulsion, the more asymmetric the spread function.

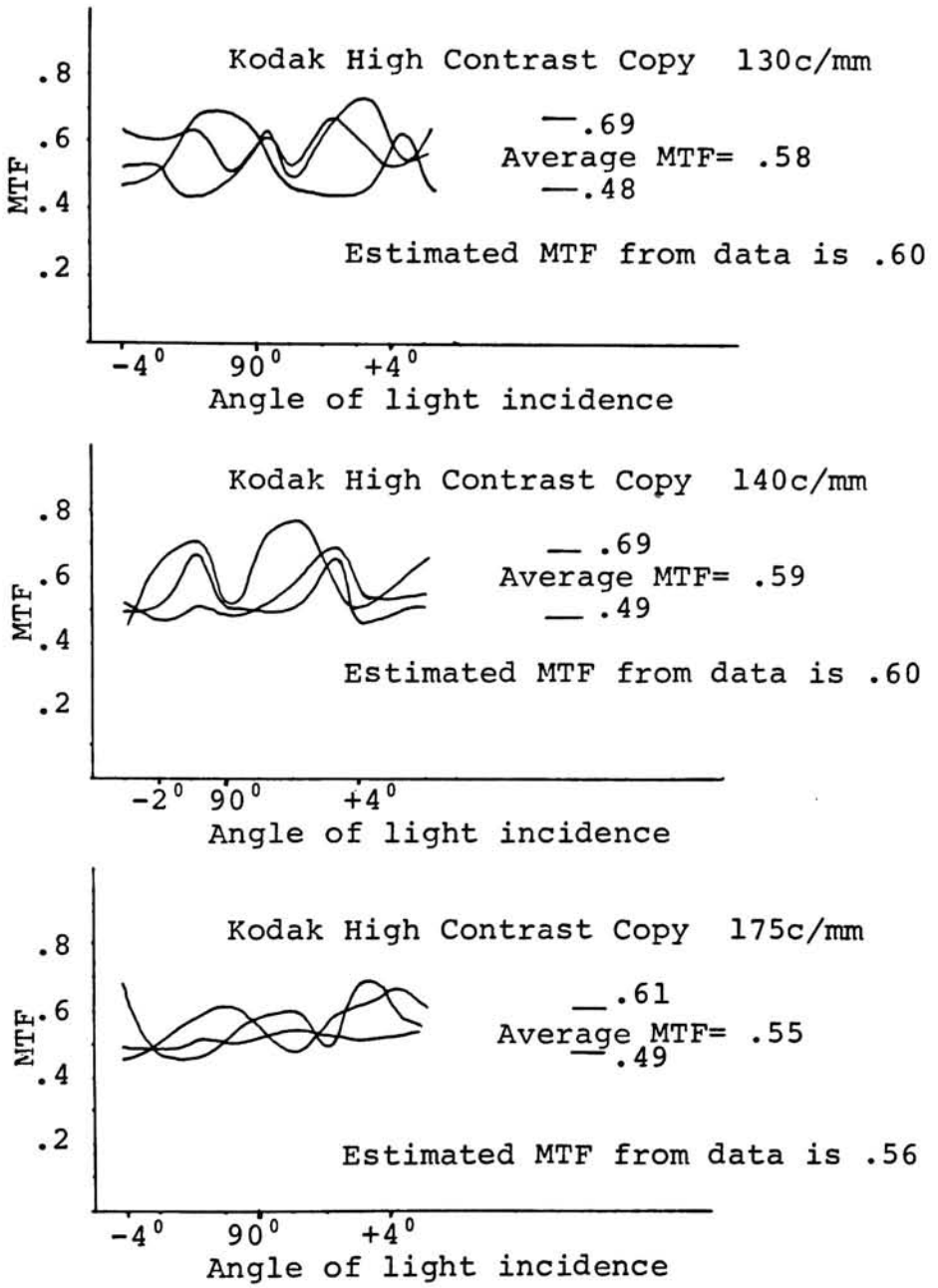

Figure 23. MTF of Kodak High Contrast Copy plotted against angle between sample and mirror. The average value closely agrees with the estimated average from Figure 21.

CONCLUSION

By employing an imageing system that simultaneously projects a sinusoidal pattern onto a film and scans the transmitted fringes, a sample's output modulation may be recorded directly. The resulting MTF shows the light distribution in the emulsion, and is independent of development effects. It represents the optical part of the frequency response of the film. This has been accomplished with a Lloyd's mirror interference system, and is used here in testing three films.

Kodak Panatomic-X produces results similar to those obtained by conventional methods. Kodalith Ortho Type 3 is evaluated without difficulty because of the elimination of the development process; and this represents an important advantage over standard procedures, since MTF determination of lithographic films is not possible by traditional methods.

Kodak High Contrast Copy film gives a wide variation in results over part of its frequency range. One explanation is that such fluctuations are a function of the angle of incidence of light.

There are a number of ways this apparatus may be improved, and the major recommendations follow. When Lloyd's mirror is used, a transparent material placed in the path of

the unreflected beam will increase that beam's optical path length, and shift the position of the zero order fringe above the edge of the mirror[14]. This allows the region on both sides of the interference maximum to be used, and reduces the effect of the fringe envelope.

Because of the type of recording method, MTF is determined from the scattered light. Any light absorbed by the silver halide grains will not be detected by the radiometer. The color of the source light will have a definite effect on the extent of scattering, dependent on the spectral sensitivity of the film being examined. Tests with other source colors would produce interesting comparisons, both in the transmission vs. time study of Figure 18, and in the MTFs obtained. Indeed with Kodalith Ortho Type 3 film, red light is not used in practical applications, so a blue or green source would definitely be more appropriate (both Panatomic-X and High Contrast Copy films are panchromatic).

A problem evident in analyzing the data is that frequencies differ slightly on each run, so no statistical analysis was applied. The spatial frequency was adjusted manually, and not known exactly until the trace of the pattern was evaluated. Future studies should employ a rotational micrometer for the mirror, allowing frequencies to be accurately preset.

Lloyd's mirror produces good quality fringes in the higher frequencies, but below about 15 c/mm, blemishes in

the mirror contribute significantly to interference distortion. Also, in this low frequency range, there may be insufficient cycles of the pattern to represent a sine wave. If data is required for low frequencies, an alternate set-up should be used, such as a Michelson interferometer. This would be a major improvement, since problems with conventional methods are most evident in this region.

The variation in MTF of High Contrast Copy film may be the result of the microscope collecting light of too specular a nature. More diffuse measurements would record much of the light which reflects sideways enough to miss the objective used in the present scheme. More tests showing MTF vs. film angle should be run, using microscope objectives of a variety of numerical apertures.

Finally, when the radiometer scans the output pattern, it reads the light transmitted by the entire film sample, not simply the emulsion. Actinic light is strongly absorbed by the anti-halation backing, and transmission of other frequencies is influenced by the color of the pelloid. These layers should be removed in future studies. Alternatively, if the emulsion is removed in a preliminary test, the MTF of the film support alone may be determined. Then the emulsion MTF is found from $MTF_{emul} = MTF_{tot}/MTF_{support}$.

LIST OF REFERENCES

1. G. C. Higgins and F. H. Perrin, Photogr. Sci. Eng., 2:73 (1958)

2. J. J. DePalmer and J. Gasper, Photogr. Sci. Eng. 16:181 (1972)

3. M. Abouelata, "Analysis and Evaluation Of Imaging Systems PPHS 741", Rochester Institute of Technology, 1972

4. J. L. Simonds, Photogr. Sci. Eng., 9:294 (1965)

5. C. N. Nelson, Photogr. Sci. Eng., 15:82-97 (1971)

6. G. Langner and R. Muller, J. Photogr. Sci., 15:9-10 (1967)

7. M. DeBelder, J. Jespers, and R. Verbrugghe, Photogr. Sci. Eng., 9:314-318 (1965)

8. H. Thiry, Photogr. Sci. Eng., 16:430-432 (1972)

9. C. B. Dach, "Light", English Universities Press, London, 1954

10. M. Born and E. Wolf, "Principles of Optics", Pergamon Press, London, 1970, Chp. 7

11. R. Welch, Photogram. Eng.;254-255 (1971)

12. Kodak Pamphlet P-49, "Modulation Transfer for Kodak Films", Eastman Kodak Co., Rochester, N.Y., 1967

13. H. Frieser, Photogr. Sci. Eng., 4:326-327 (1960)

14. R. A. Houstoun, "A Treatise on Light", Longmans, London, 1915, pg. 138

APPENDIX A

APPENDIX A

For two functions $f_1(t)$ and $f_2(t)$, the convolution $f(t)$ is defined by the integral

$$f(t)=\int f_1(\eta)\, f_2(t-\eta)\, \partial\eta \qquad \text{(A1)}$$

and is expressed $f(t)=f_1(t)*f_2(t)$. Equation A1 states that the convolution of two functions $f_1(t)$ and $f_2(t)$ is found by shifting $f_2(\eta)$ to the right by a quantity t, reflecting $f_2(\eta-t)$ about $\eta=t$, and multiplying the reflected function by $f_1(\eta)$. Integrating over the extent of the two functions gives $f(t)$. The process is communatative, so either function may be folded.

One of the important properties of the convolution integral is its relation to the Fourier transform. This property states that the Fourier transform of the convolution of two functions is the product of the Fourier transforms of the individual functions. This is known as the Time Convolution Theorem, and is shown by the following.

If the Fourier transform of $f_1(t)$ is $F_1(\omega)$, then

$$F_1(\omega)=\int_{-\infty}^{\infty} f_1(t)\, e^{-i\omega t}\, \partial t \qquad \text{(A2)}$$

where ω is the spatial frequency in radians/mm. It follows that the transform of $f_1(t)*f_2(t)$ is

$$F(\omega)=\int_{-\infty}^{\infty}\left[\int_{-\infty}^{\infty} f_1(\eta)\, f_2(t-\eta)\right]\, \partial\eta e^{-i\omega t}\, \partial t$$
$$=\int_{-\infty}^{\infty} f_1(\eta)\, \partial\eta \int_{-\infty}^{\infty} f_2(t-\eta)\, e^{-i\omega t}\, \partial t\,.$$

$$\text{But} \int_{-\infty}^{\infty} \partial t f_2(t-\eta) e^{-i\omega t} = F_2(\omega) e^{-i\omega\eta}$$

$$\text{Therefore} \quad F(\omega) = \int_{-\infty}^{\infty} F_2(\omega) f_1(\eta) e^{-i\omega\eta} \partial\eta$$

$$F(\omega) = F_1(\omega) F_2(\omega) \ . \tag{A3}$$

APPENDIX B

APPENDIX B

As the spatial frequency of the interference pattern decreases, fewer and fewer cycles are visible. The angle that the light from the source makes with the mirror becomes so small that the region of interference,d,produces only a few cycles. In FIGURE 24, the mirror has a fixed length L=200mm. For small angles, $d=\theta L$. We wish to determine if the fringe quality at frequency ν=10 cycles/mm is acceptable. Now $\nu=2\theta/\lambda=10$ where λ is the wavelength of the source, $6.3\text{x}10^{-4}$ mm. So $\theta=3\text{x}10^{-3}$, giving y=.6mm. Therefore, at this frequency, 6 cycles are visible.

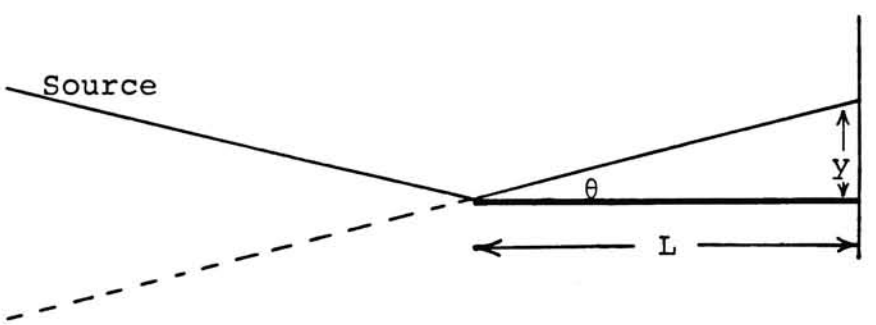

Figure 24. Calculation of region of interference, y, in Lloyd's mirror arrangement.

To test the quality of the fringes, the situation may be treated as a cosine function restricted to a window of width y. The function in Figure 25 may be expressed as

$$f(t)=u(t)\ \cos\omega_0 t \tag{B1}$$

where $$u(t)=\begin{cases} 1 & |t|\leq \tfrac{1}{2}y \\ 0 & |t|>\tfrac{1}{2}y \end{cases}.$$

To see how closely it resembles cos $\omega_0 t$, we find the Fourier transform of f(t), and compare it to the transform of cos $\omega_0 t$.

$$\mathcal{F}\left[f(t)\right]=\mathcal{F}\left[u(t)\ \cos\ \omega_0 t\right]$$
$$=\tfrac{1}{2}\int u(t)e^{-i(\omega-\omega_0)t}\partial t + \tfrac{1}{2}\int u(t)e^{-i(\omega+\omega_0)t}\partial t.$$

Now if $\mathcal{F}\left[u(t)\right]=F(\omega)$

then $\mathcal{F}\left[f(t)\right]=\tfrac{1}{2}F(\omega-\omega_0)+\tfrac{1}{2}F(\omega+\omega_0)$.

Finding F(ω)

$$\mathcal{F}\left[u(t)\right]=\int u(t)e^{-i\omega t}\partial t=\int e^{-i\omega t}\partial t$$
$$=d\ \frac{\sin(\omega y/2)}{\omega y/2}.$$

Therefore $\mathcal{F}\left[f(t)\right]=\tfrac{1}{2}F(\omega-\omega_0)+\tfrac{1}{2}F(\omega+\omega_0)$

$$\mathcal{F}\left[f(t)\right]=\tfrac{1}{2}d\ \frac{\sin\ \tfrac{1}{2}y(\omega-\omega_0)}{\tfrac{1}{2}y(\omega-\omega_0)}+\tfrac{1}{2}d\ \frac{\sin\ \tfrac{1}{2}y(\omega+\omega_0)}{\tfrac{1}{2}y(\omega+\omega_0)}. \tag{B2}$$

Equation B2 describes two sinc functions, about $\omega=\omega_0$, and $\omega=-\omega_0$. $\mathcal{F}\left[f(t)\right]$ is plotted in Figure 26.

The transform of cos $\omega_0 t$ is two delta functions centered at ω_0 and $-\omega_0$, and the approximations in Figure 26 compare favorably with this. So down to 10 cycles/mm, it can be concluded that the interference fringes produced are of acceptable quality.

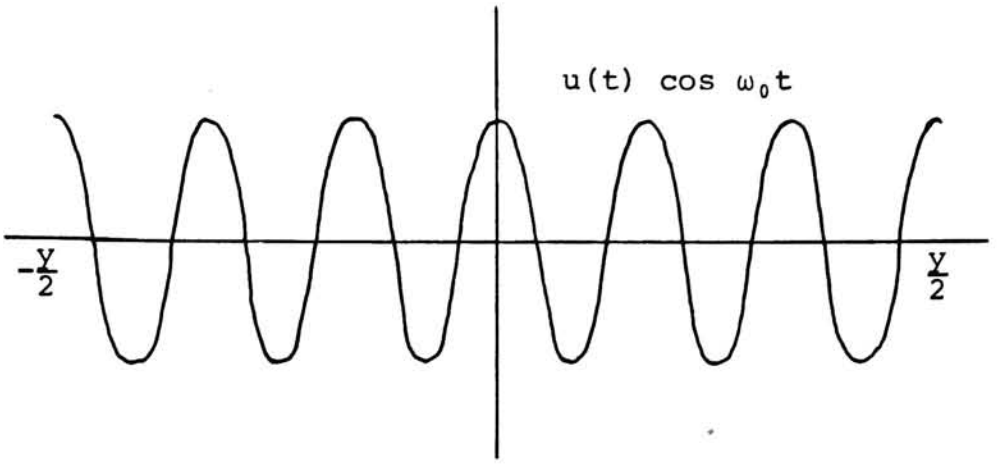

Figure 25. A true cosine wave limited by a window of width y.

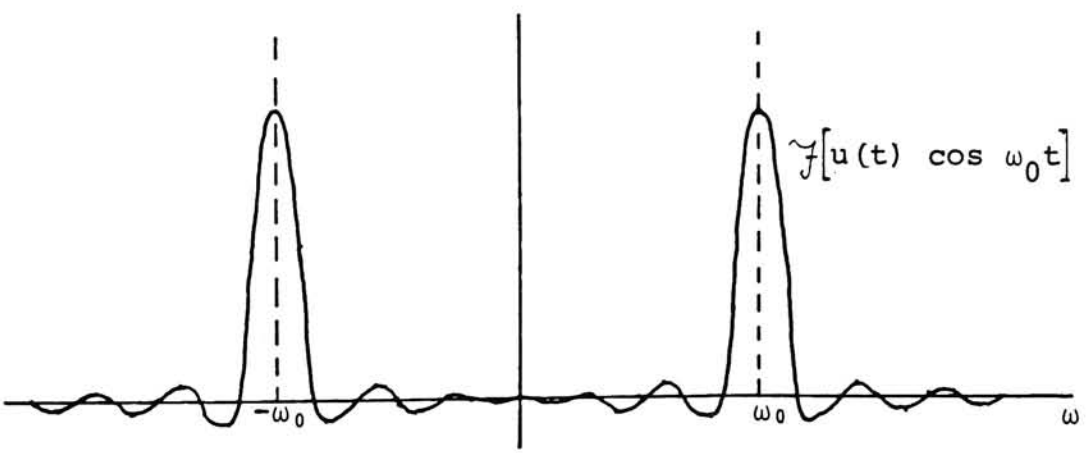

Figure 26. Fourier transform of limited cosine function is two sinc functions about $\omega=\omega_0$ and $\omega=-\omega_0$.